Response to the Referees

Kilometric wave emission observed on pre-midnight side in the vicinity of the Earth's magnetic equatorial plane at 1-2 L-Shell

First of all, we thank both reviewers for their constructive comments and suggestions. In the title, we have written 'Kilometric wave emission' instead of 'terrestrial kilometric radiation', and indicated where DEMETER detected such radiation. In the upgraded version we have re-considered and re-written essentially the Section 3 taking into consideration the reviewer comments. It is evident that the confusions between DEMETER kilometric wave emission and the terrestrial kilometric radiation are due to three main reasons: spectral beam, i.e. 'Christ tree', are similar, the parallel bands and the beaming around the magnetic equatorial plane. In the discussions Section, i.e. Section 3, we have summarized the main results and insisted on one side, on the spectral features of the kilometric wave emissions and on the other side on the similarities and the discrepancies between the DEMETER kilometric emission and the terrestrial kilometric radiation. The Z-mode is considered as a generation mechanism candidate. Our responses to referee are listed below.

Response to Referee #1

Reviewer1: The authors state that kilometric continuum (KC) is observed by the DEMETER spacecraft, which is at an altitude of ~700 km. The scatter plot in Figure 4 shows the bulk of the emissions occurring below 100 kHz. At 100 kHz the plasma density is ~120 cm-3. Since KC is a free space mode radiation its frequency (f) must be above FPE or FR [eg. Shaw and Gurnett, 1980, Kennel et al., 1987]. I don't know the DEMETER location for Figure 1 so used 2 magnetic field strengths in the table below.

$N_E(cm^{-3})$	B(nT)	F_{PE} (kHz)	F_{CE} (kHz)	F_R (kHz)	F_L (kHz)
10000	30000	900	839	1413	573
1000	30000	284	839	927	87
100	30000	90	839	849	9
10000	20000	900	559	1222	662
1000	20000	284	559	679	119
100	20000	90	559	573	14
The cutoffs F_R is f where R=0, F_L is f where L=0; R&L are from Stix [1962] F_{PE} -plasma frequency, F_{CE} -electron cyclotron frequency.					

The authors suggest that the emissions observed by DEMETER could be related to plasmaspheric plumes. For one to believe these emissions observed by DEMETER are free-space KC, a plasmaspheric drainage plume/channel would have to extend down to ~700 km altitude with minimum densities of say ~ 100 cm-3 or less at that altitude; an altitude where ~ 104 to 4x104 cm-3 is common near the equator. Looking at Figures 2 and 3 of Chen et al., [2018] NE dropping below 104 cm-3 on the nightside or dayside around the equator is rare. So, if DEMETER is frequently seeing this emission around the equator then I don't believe these emissions are free-space. Z-mode radiation occurs at f between FL and FUHR (upper hybrid resonance f) the authors need to check if this radiation could be Z-mode. A key issue must be resolved, before the reviewer can accept this paper for publication.

MAJOR COMMENTS

R1_A: A key issue must be resolved, before the reviewer can accept this paper for publication. Since this is a major claim that DEMETER detects KC, a detailed event analysis should be given in the paper that demonstrates the radiation is free space mode. You have not convinced me that your type 1&2 events are free space radiation. I suggest that you show one of more example spectrograms of events with the frequency of the & FPE & & FR & FL & FCE lines overlaid on the spectrogram. This will give the reader a feeling of whether or not the radiation is free-space. If ISL Langmuir probe paper Lebreton et al. [Planetary and Space Science 54 (2006) 472–486] data is not available for any of your events, you could try IAP or infer the plasma density from the E/B ratio using data below 17.4 kHz, assuming you can identify the wave mode and the E&B measurements are reliable. 100 per cc might be the threshold of ISL so f(l=0) & fpe & fuhr would be a upper limit.

A1_A: As suggested by the referee, we have checked and found that the considered kilometric wave emissions can't a free space radiation. In all events the gyrofrequency (FCE) is above the frequency associated to the LF kilometric emission. In Fig.1 or Fig.2 the gyro-frequency is indicated.

R1_B: If you can correlate some of your events with KC events observed by GEOTAIL PWI. The GEOTIAL PWI 24 hr survey plots are located at http://space.rish.kyotou.ac.jp/gtlpwi/. I see no KC in the GEOTAIL PWI spectrograms for the 2 days given in your paper, of course GEOTAIL could be at the wrong LT or the KC generated at low RE does not always escape the plasmasphere/ionosphere.

A1_B: GEOTAIL orbits were mainly far, at least 10 RE, and on the day side. We have checked the PWI dynamic spectra for the investigated period and did not find comparable spectral features as recorded by DEMETER. This may be due to the distance of the satellite which is bigger than 5 RE.

R1_C: On your spectrogram plot please indicate where the IGRF (or similar) model field aligned magnetic minimum crossing occurs. If centered about the Type 2 emissions then this would cast doubt in my opinion about the emissions being KC.

A1_C: As suggested by the referee, we have indicated in Fig.1 and Fig.2 the gyrofrequency.

R1_D: No discussion of the interpretation of the harmonics of type 2 is given. Looking at the type 2 in Figure 1, the spacing between the harmonics is ~25 kHz. Using a simple dipole and standard continuum emission model this places the equatorial source at about ~3.2 RE, with a sharp plasma gradient, with Ne extending up to at least (fpe=600 kHz) ~4500 cm-3 at that location. Fpe at 600 kHz at ~3.2 RE is at the upper range of observed plasmaspheric plasma frequencies at ~3.2 RE, further casting doubt in my opinion.

A1_D: We totally agree concerning the harmonics of type 2. The frequency spacing of 25 kHz of Figure 1, recorded mainly in the southern part of magnetic equator, is variable from one event to another. This structured component disappears when we consider all events, i.e. as can see in the first panel of Fig.4. However in the northern magnetic equatorial plane, the frequency interval is, on average, about 150 kHz at magnetic latitude 20°N.

R1_E: It is not clear to me if harmonic spacing of ~25 kHz can be explained in terms of local plasma conditions and/or non-linear processes. Because FCE is large I would like to see at least one the spectrogram of the entire ICE frequency range out to 3.25 Mega-Hz.

A1_E: We have added in Fig.1 and Fig.2 an overview (i.e. total frequency range) and a zoomed part (i.e. from few kHz up to about 900 kHz) for the two examples.

R1_F: Have you to tried to correlate Type 2 with the particle measurements (IAP, ISL, IDP)? It's important to understand these emissions. Have you searched for other explanations for these emissions? Could this be an example of instrumental spherical probe pre-amp oscillations due to localize plasma conditions?

A1_F: In reality, we did not check the particle measurement on aboard DEMETER. This may be done in further investigation of this work. Of course, we did not try to search for other explanations since we thought that we deal with terrestrial kilometric radiation particularly because of the spectral beam. Concerning the instrumental influence, Bertherlier (PI of ICE experiment) did not address such instrumental effects in his paper (i.e. Berthelier et al., 2006). The frequency bandwidth is not constant but variable from one event to another.

OTHER COMMENT

R1_G: Free-space or Z-mode emission in an equatorial plasma bubbles might be another possibility instead of drainage plumes. Equatorial bubbles are observed by DMSP on about 1 out 8 orbits [Huang et al., JGR 2001] whether the internal density of bubbles can be low enough to accommodate the DEMETER observations is not clear.

A1_G: We though to the drainage plumes because of the development of the emission beam in the case of the terrestrial kilometric radiation. In the upgraded version, we only refer to the source location as reported by Green & Boardsen (2006) and avoid the confusion between both kilometric emissions.

R1_H: Line 28. 'We use a manually technique which consists to follow and to save with the PC-computer mouse'. Instead of manual selection did you try an automated selection method. Looking at Figure 1, it seems like automated selection followed by visual inspection of those selections might save one time, this would allow you to scan a larger time interval.

A1_H: The manual technique has been adapted because of: (a) the weak intensities of kilometric wave emission when compared to AKR and also to the instrumental noise level, (b) the phenomenological aspects of this emission where we have attempted to classify/distinguish other spectral components observed at mid-latitude and sub-auroral regions and (c) the presence of LF transmitters which are overlapping the investigated kilometric wave emission.

R1_I: You don't give enough information about your survey. Start/stop dates that your survey covered. We looked a X nightside equatorial crossings finding Y events? We looked a X dayside equatorial crossings finding Y events?

A1_I: In the paper, we have indicated the probability of occurrence of such kilometric wave emissions observed only on the night-side of the Earth. We found that the crossing of the magnetic equatorial plane by DEMETER is usually followed by the detection of kilometric wave emissions, as displayed in Fig.4. The difference from one orbit to another is the intensity level of the emission and also the frequency bandwidth which is found in the range between few kHz and 800 kHz.

R1_J: Where these emissions not observed before 2010? If so why, or did you not look before 2010?

A1_J: We started in the beginning of 2010 because of the low solar activity. We followed the work of Kuril'chik et al. (2001) who reported that the terrestrial kilometric radiation is regularly observed during quiet solar activity.

R1_K: Figure 1 is not of publication quality. I would also include a dayside example, maybe 2 dayside and 2 nightside examples, with better annotation as described earlier in the review.

A1_K: As suggested by the referee, we have considered two examples with better annotations. We have no dayside events.

R1_L: Figure 2 Lack of clarity in how the histogram is computed: for example, looking at Figure 1 at 14:01:40 are all harmonics summed in a given latitude bin? I would make a weighted histogram instead, summing the weights in each latitude bin. For example if you selected 800 points in Figure 1, then I would weight each selection by 1/800 for that equatorial crossing.

A1_L: We attempt in this paper to provide a global view of the occurrence of all events. The use of manually method is not adequate for 'weighting' the bin in latitude and longitude. For the data processing, we did not use conditions on: (a) the time and frequency spacing between two points, and (b) on the intensity level. We have emphasized on the spectral pattern of the emissions like the fluctuation in time and frequency, and the variable frequency bandwidth.

R1_M: Why not split histogram into day/night? Scatter plot of power versus frequency might be revealing. An annotated spectrum at the center of Type 2 would also be helpful. Power level (defined as square root of the power spectral density)

A1_M: We observed the kilometric wave emission only when DEMETER was on the night-side. Fig.4, 5, 6, and 7 displayed the dependence of the emission frequency on the power levels. We have considered three intensity levels associated to the three maxima derived from the second panel of Fig.3. The power level has been corrected and expressed as $\mu V\ m^{-1}Hz^{-1/2}$.

R1_N: Figure 3: include legend of what the 3 colors correspond too, don't just say it in the text, this makes it hard for the reader.

A1_N: The colors associated to the power levels are corrected and indicated in the new legend of Fig.3.

R1_O: Figure 4: include legend of what the 3 colors correspond, don't just say it in the text. Why not split into day/night?

A1_O: We also precise in the new legend of Fig.4 the corresponding power levels.

R1_P: A scatter plot for Type 2 of the frequency spacing of harmonics versus frequency of harmonic might be revealing. From standard theory this can be used to estimate the fc/fp ratio at the source under the assumption that the density gradients are sharp.

A1_P: We have previously indicated that the frequency bandwidth is variable. The assumption about the density gradients have been discussed in the upgraded version if the observed emission is the terrestrial kilometric radiation. The fc/fp ratio may be applied if the plasma frequency is higher than the gyrofrequency frequency. It is not the case in this study.

References

Chen, C. Y., Liu, T. J. Y., Lee, I. T., Rothkaehl, H., Przepiorka, D., Chang, L. C., et al. (2018). The mid-latitude trough and the plasmapause in the nighttime ionosphere simultaneously observed by DEMETER during 2006–2009. Journal of Geophysical Research: Space Physics, 123, 5917–5932. https://doi.org/10.1029/2017JA024840

Huang, C. Y., Burke, W. J., Machuzak, J. S., Gentile, L. C., and Sultan, P. J. (2001), DMSP observations of equatorial plasma bubbles in the topside ionosphere near solar maximum, *J. Geophys. Res.*, 106 (A5), 8131– 8142, doi:10.1029/2000JA000319.

Kennel, C. F., Chen, R. F., Moses, S. L., Kurth, W. S., Coroniti, F. V., Scarf, F. L., and Chen, F. F.(1987), *Z* mode radiation in Jupiter's magnetosphere, *J. Geophys. Res.*, 92(A9), 9978– 9996, doi:10.1029/JA092iA09p09978.

Shaw, R. R., and Gurnett, D. A. (1980), A test of two theories for the low frequency cutoffs of nonthermal continuum radiation, J. Geophys. Res., 85(A9), 4571– 4576, doi:10.1029/JA085iA09p04571.

Response to the Referees

Kilometric wave emission observed on pre-midnight side in the vicinity of the Earth's magnetic equatorial plane at 1-2 L-Shell

First of all, we thank both reviewers for their constructive comments and suggestions. In the title, we have written 'Kilometric wave emission' instead of 'terrestrial kilometric radiation', and indicated where DEMETER detected such radiation. In the upgraded version we have re-considered and re-written essentially the Section 3 taking into consideration the reviewer comments. It is evident that the confusions between DEMETER kilometric wave emission and the terrestrial kilometric radiation are due to three main reasons: spectral beam, i.e. 'Christ tree', are similar, the parallel bands and the beaming around the magnetic equatorial plane. In the discussions Section, i.e. Section 3, we have summarized the main results and insisted on one side, on the spectral features of the kilometric wave emissions and on the other side on the similarities and the discrepancies between the DEMETER kilometric emission and the terrestrial kilometric radiation. The Z-mode is considered as a generation mechanism candidate. Our responses to referee are listed below.

Response to Referee #2

Reviewer2: This paper reports observation of LF waves which might be generated at the plasmapause and propagate to the low-altitude equatorial region. The observation results are interesting and raised some important problems of propagation characteristics of the LF waves in the plasmasphere. I have some comments on the paper.

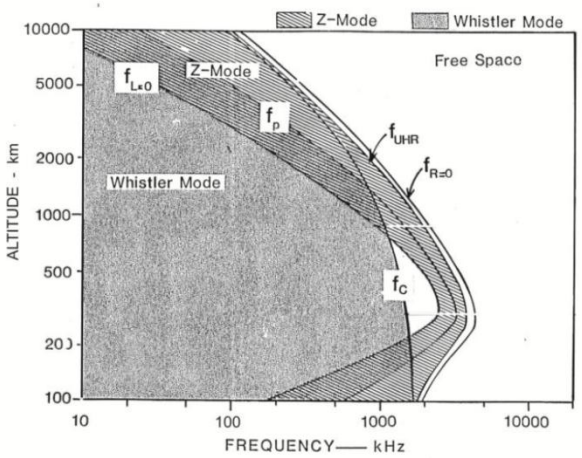

R2_A: 1. In the manuscript, the authors do not mention an important point, that is, the observed LF waves by DEMETER are "whistler mode waves". I attached a diagram (drawn by myself) which shows the characteristic wave-mode in the frequency range of 10 kHz-2 MHz in the altitude range of 100-10000km. It is obvious that the ICE/DEMETER instrument can detect only the whistler mode waves within the observation frequency range up to 3.5 MHz at the altitude of DEMETER (about 700km). Thus, the observed waves by DEMETER are not free-space mode but R-X mode of whistler waves trapped in the plasmasphere. When the authors consider the LF wave propagation from the

source region near the plasmapause to the low-altitude equatorial region, they should take into account the propagation characteristic of whistler mode waves with respect to the magnetic field.

A2_A: We agree with the referee suggestion concerning the whistler mode waves as a physical process at the origin of this emission. The attached diagram, provided by the referee, leads to explain the observed frequencies and their corresponding altitudes. In the upgraded version, we report about new references concerning whistler mode waves and particularly the Z-mode which may be observed in the vicinity of the magnetic equatorial plane.

2_B: 2. I recommend considering the mode conversion of original radiations, which are probably Z-mode or upper hybrid mode radiation generated around the plasmapause, to whistler mode waves. And the observed kilometric radiation at DEMETER can be whistler mode wave. However, in this case, it becomes difficult and needs some suitable idea to interpret the "beam pattern" derived from the authors' study, because the whistler mode wave tends to propagate along the magnetic field. This is the interesting point that authors raised.

A2_B: We did not change too much in the content of the Section 2 when it is compared to the previous one. We have mainly derived the observational parameters particularly the variation of the power level versus the frequency and the magnetic latitude. In Section 3, we have attempted to explain the similarities and the discrepancies between the DEMETER kilometric emission and the well-known terrestrial kilometric radiations.

R2_C: 3. In the text, the authors say that the type1 is trapped component and the type2 is escaping component. What is the reason? Usually, the term of trapping/escaping is used in the case of free-space mode propagation in the magnetosphere.

A2_C: It is clear from the dynamic spectrum of kilometric wave emission that we deal with two components. The spectral shapes, as shown in Fig.5, are found to be similar to those associated to the terrestrial kilometric emission. For this reason we have considered the trapped (Type 1) and escaping (Type 2) emission taking into consideration the frequency boundaries around 50 kHz. Such spectral patterns are addressed and discussed in Section 3.

R2_D: 4. The authors distinguished two varieties of emission: "Type 1 appears as a narrow continuum with an instantaneous bandwidth of about 2 kHz at frequencies less than 50 kHz, and displays negative and positive frequency drifts when the satellite is approaching or leaving the equatorial plane, respectively. Its frequency drift rate is weak and in the order of 0.2 kHz/s. Type 2 is composed of parallel narrow-bands in a frequency above 50 kHz and up to 800 kHz."
I agree the presence of Type1 and Type 2 radiations, but do not agree to use mixed data of Type1 and Type2 in the analysis of figures 2-6. I suggest that they should be separately analyzed, because the different characteristics of type1 and 2 suggest the different source mechanism and/or different propagation pass.

A2_D: In the upgraded version, we have described both types of emissions. However, we don't consider them as trapped and escaping emissions. We have attempted to insist on the source regions of both components as discussed in Section 3. Further surveys of ICE observations may allow a better characterization of each component by considering a longer period of investigations, at least one year.

R2_E: 5. The authors found structured emissions in the LF waves, and classified into two categories: "In the northern hemisphere, five components in the frequency ranges of few kHz - 50 kHz, 70 kHz - 130 kHz, 170 kHz - 250 kHz, 280 kHz -340 kHz and 380 kHz- 420 kHz.
In the southern hemisphere, four components in the frequency bands: of 200 kHz - 320 kHz, 320 kHz - 450 kHz, 450 kHz - 570 kHz, and 570 kHz - 670 kHz." The reader will imagine that these bands are showing the higher harmonic relation. In fact, as shown in Figure 1, an individual event shows fine harmonics. And, one can easily infer the fundamental frequency from the harmonic relation, and then can suppose the source altitude of the emission assuming the distribution of gyrofrequency and plasma frequency. I suggest to add discussion on this matter in the text.

A2_E: In Section 3, we have suggested the probable source regions of the kilometric wave emissions as a micro-scale region in the inner plasmasphere. In the new Fig.9, we have attempted to display how the Z-mode frequency is delimiting the source altitude.

R2_F: 6. minor comments: *p1, line17 seventeens should be seventies, *p2, line 13 plasmasphere should be magnetosphere.*Fig 6 vertical axis is wrong. * Unpublished paper should not be included in References.

A2_F: Minor comments are considered in the upgraded version. Unpublished references (i.e. Boudjada et al., EGU09 & Boudjada et al., EGU14) have been deleted from the text and the reference list.

~~Terrestrial~~ Kilometric ~~wave emission radiation~~ observed on pre-midnight side in the vicinity of the Earth's magnetic equatorial plane at 1-2 L-Shell

Mohammed Y. Boudjada[1], Patrick H.M. Galopeau[2], Sami Sawas[3], Valery Denisenko[4,5], Konrad Schwingenschuh[1], Helmut Lammer[1], Hans U. Eichelberger[1], Werner Magnes[1], and Bruno Besser[1]

[1]Space Research Institute, Austrian Academy of Sciences, Graz, Austria
[2]LATMOS-CNRS, Université Versailles Saint-Quentin-en-Yvelines, Guyancourt, France
[3]Institute of Communications and Wave Propagation, University of Technology, Graz, Austria
[4]Institute of Computational Modelling, Russian Academy of Sciences, Krasnoyarsk, Russia
[5]Siberian Federal University, Krasnoyarsk, Russia

Correspondence: M.Y. Boudjada (mohammed.boudjada@oeaw.ac.at)

Abstract. The ICE experiment onboard the DEMETER satellite recorded kilometric wave emissions in the vicinity of the magnetic equatorial plane. Those radiations were observed in the beginning of the year 2010 on the night-side of the Earth and rarely on the day-side. We distinguish two components one appears as a continuum between few kHz and up to 50 kHz and the other one from 50 kHz to 800 kHz. The first component exhibits positive and negative frequency drift rates in the southern and northern hemispheres, at latitudes between 40° and 20°. The second component displays multiple spaced frequency bands. Such bands mainly occur near the magnetic equatorial plane with a particular enhancement of the power level when the satellite latitude is close to the magnetic equatorial plane. We show in this study ~~that both components are linked to the terrestrial non-thermal kilometric radiation. Those two components are the trapped and the escaping terrestrial non-thermal kilometric radiation. Above 150 kHz, we have found that the escaping emissions are mainly extended in frequency in the southern hemisphere and in geomagnetic latitude in the opposite hemisphere. DEMETER low altitude orbits lead to describe the frequency and the time evolution of this terrestrial radiation particularly on the evening sector at L-Shell of about 2. We show the dependence of the power intensity on the emission frequency, and provide a hint on the location of the source region and its relation to the Earth's plasmasphere. It is shown that the so-called 'Christmas-tree' pattern associated to the terrestrial kilometric radiation may be associated to the plume and channel generated in the~~ ~~pre-midnight sector of the plasmasphere~~ the similarities and the discrepancies between DEMETER kilometric emission and the well-know terrestrial kilometric radiation. We believe that both emissions are the signatures of the radio sources localized in the inner and outer parts of the plasmasphere. The hollow cones of the DEMETER kilometric wave emissions are oriented towards the Earth's ionosphere, and not the magnetosphere. We suggest that such emissions are associated to Z-mode trapped region only detectable by electric field experiment onboard low Earth orbiting satellite at altitudes less than 700 km.

1 Introduction

A variety of radio waves have been detected in the near Earth's space environment in the ~~seventeens~~ seventies. Imp 6 satellite radio measurements have allowed the identification, for a first time, of a weak continuum associated to the Earth's magnetosphere. The continuum power level was found to be below the cosmic noise level at frequencies of about 100 kHz with a low frequency of 30 kHz (Brown, 1973) which was considered to be produced by solar wind local plasma frequency. Another continuum component but more intense have been identified at even lower frequencies, between 5 and 20 kHz (Gurnett and Shaw, 1973). This

radiation is found to occur at frequencies smaller than the local plasma frequency of the solar wind. Gurnett (1975) showed that these two types of emission belong to a single non-thermal continuum spectrum, one 'trapped' and the other 'escaping'. The first component has frequencies lower than about 30 kHz which correspond to the magnetopause plasma frequency, and the second one has frequencies above this limit. Kurth et al. (1981) showed using ISEE 1 satellite quite temporal and spectral differences between both components. The observed differences are interpreted as the effect of the cavity on the 'trapped' component. Also high resolution spectrograms made evident the presence of numerous narrow-band emissions for the 'escaping' component.

Recent missions like CLUSTER, GEOTAIL, IMAGE and INTERBALL-1 provide new observations of the terrestrial nonthermal continuum. Hashimoto et al. (1999, 2006) reported about a new component at frequencies of 100 to 800 kHz detected when GEOTAIL satellite was at 10 to 30 R_E inside the Earth's ~~plasmasphere~~ magnetosphere. About one hundred events were recorded during the period from 01^{st} Jan. to 31^{st} Dec. 1996. Events were found to occur on the dayside/evening sectors and within about 10° of the magnetic equator. Kuril'chik et al. (2001, 2007) reported events of kilometric continuum recorded by INTERBALL-1 satellite very close to the Earth (1.6 to 2.4 R_E) with a high spectral resolution (10 kHz and 0.2 sec) at two frequencies 252 kHz and 500 kHz. Authors showed that the 'continuum' emission has a rather impulsive character, and a dependence of the beam widths on the solar activity. The polar orbit of the IMAGE satellite allowed finding that the nonthermal continuum radiation extends from about 29 kHz to about 500 kHz and forming a 'Christmas tree' pattern, nearly symmetric about the magnetic equator (Green and Boardsen, 2006). IMAGE satellite observations showed that the kilometric continuum is confined to a narrow latitude range of about 15°. The source region of the kilometric continuum is found in the plasmapause within notch structures co-rotating with the Earth (Green et al., 2004). First CLUSTER non-thermal continuum observations were reported by Décréau et al. (2001). Direction finding technique, based on antenna spin modulation, allowed localizing the source regions in the plasmapause (Décréau et al., 2004) confirming IMAGE observations. CLUSTER tetrahedral configuration of four identical satellites allowed the analysis of specific type of nonthermal continuum. Hence Grimald et al. (2008) showed in the nonthermal emissions the presence of spectral peaks organized as several banded emissions with a frequency interval nearby the gyrofrequency at the source. Also details on the wave spectral signature was investigated by El–Lemdani Mazouz et al. (2009) particularly the splitting in fine frequency bands. Another type called 'nonthermal continuum patches' were found to occur within a relatively short time and over a wide frequency range (Grimald et al., 2011). Authors showed that 'patches' events represent 25% of the total nonthermal emissions recorded in one year.

Physical mechanisms at the origin of the terrestrial nonthermal continuum were first proposed by Frankel (1973) who considered gyro-synchrotron radiation linked to energetic electrons. Gurnett and Frank (1976) made evident correlation between continuum radiation and 1 to 30 keV electrons. Such electrons injection let to intense electrostatic waves nearby the upper hybrid resonance frequency. A linear conversion model was suggested by Jones (1976,1977) where electrostatic waves in the presence of a density gradient would convert into ordinary mode radio waves. In the source region, the density gradient must be nearly perpendicular to the magnetic field. This model predicts a beamed radiation outward in two meridionals beams at angles of $\gamma = \pm arctan(fc/fp)^{1/2}$ with regard to the magnetic equator. Those angles are depending on f_p the electron plasma frequency and f_c the cyclotron frequency. Also Jones model expects that the generated O-mode emission should be left-hand polarized. The beamed radiation and the O-mode polarization have been confirmed, respectively, by Jones et al. (1987) and Gurnett et al. (1988).

In this paper, we analyze the ~~terrestrial non-thermal~~ kilometric wave radiation observed by ICE/DEMETER experiment in the beginning of the year 2010. The characteristics of this radiation, essentially the spectral features and the spatial occurrence are described in Section 2. Discussion of the outcomes is detailed in Section 3 where principally our results are combined to previous ones. Summary of the main results are given in Section 4.

2 Kilometric radio emission

2.1 Overview of HF/ICE observations

We consider in this study the space observations provided by the DEMETER microsatellite. The aim is the analysis of particular spectral features recorded by the ICE experiment in the beginning of the year 2010, i.e. January, February and March. The ICE instrument allows a continuous survey of the electric field over a wide frequency range, from few Hz up to about 3.5 MHz (Berthelier et al., 2006). The electric field component is determined along the axis defined by two sensors. The satellite sun-synchronous half-orbit duration is about 40 min and covering invariant latitude between -65° and +65°. The DEMETER satellite orbits are associated to two fixed local times (LTs), at about 10 LT and 22 LT. We use in this investigation the survey mode of the ICE experiment covering the frequency range between few kHz and 3.5 MHz, called hereafter HF-band. The radio wave emissions are alternately recorded on the day- and night-sides of the Earth corresponding respectively to down and up half-orbits. However the main radiations investigated in this paper are observed on the night-side, and rarely on the day-side. Generally the ICE HF-band dynamic spectra allow distinguishing three kinds of spectral emissions depending on the satel-

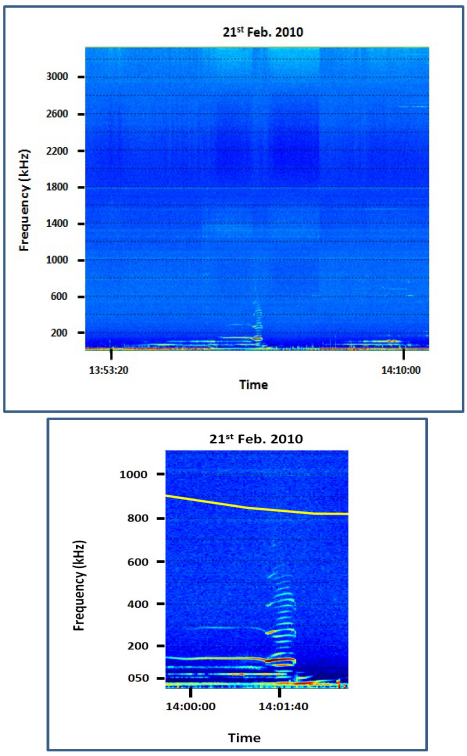

Figure 1. ~~Dynamic spectrum recorded by the ICE/DEMETRE experiment where two components, i.e. Types I and II, are indicated. This event was observed on 10^{th} January 2010.~~ Example of kilometric wave emission recorded by the ICE/DEMETER on 21^{st} Feb. 2010. The first panel displays an overview of the dynamic spectrum in the frequency range from few kHz to 3.5 MHz. The second panel shows a zoomed part for the event in the frequency bandwidth between few kHz and 1100 kHz. The gyro-frequency is indicated by the yellow curve.

lite geographical latitudes. The first one is recorded close to the sub-auroral regions at latitudes between 50° and 60°; it mainly concerns the auroral kilometric radiation described by ~~Boudjada et al. (2009, 2014) and~~ Parrot and Berthelier (2012). The second are mainly ground-based transmitters, low frequency (LF) radiation, appearing at mid-latitudes between 50° and 20°, in both hemispheres (e.g., Parrot et al., 2009; Boudjada et al., 2017).

The third kind of emission is a kilometric wave radiation occurring in the vicinity of the equatorial magnetic plane at low latitudes. Hereafter we focus on the analysis of the kilometric radiation in particular the spectral characteristics, the magnetic latitude and the power intensity occurrence. Also the dependence of the power level on the frequency and the magnetic latitude is considered. We use a manually technique which consists to follow and to save with the PC-computer mouse the frequency and the temporal evolution of the ~~terrestrial kilometric~~ radiation. The saved parameters are the observation time (UT hours), the frequency (kHz) and the power level (~~$\mu V m^{-2} Hz^{-1}$~~ $\mu V m^{-1} Hz^{-1/2}$). The collected points are later combined with the satellite orbital parameters like the magnetic latitude and the L-Shell.

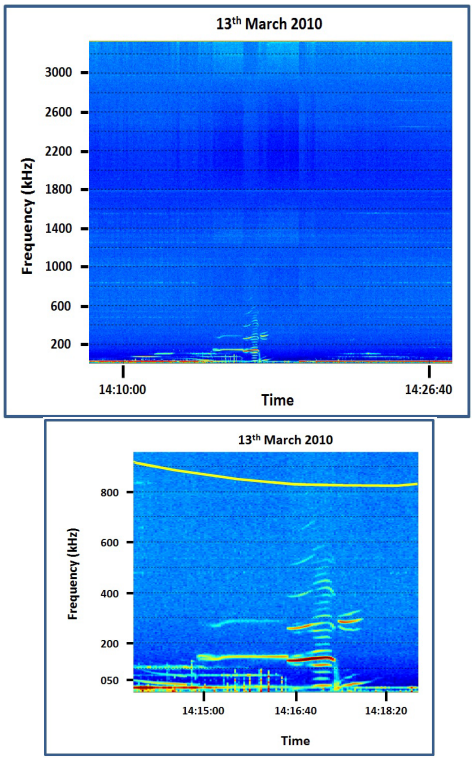

Figure 2. ~~Occurrence of terrestrial kilometric emissions in magnetic latitude (Degree) and in power level ($\mu V m^{-2} Hz^{-1}$)~~ Like in Fig.1 for an event recorded by DEMETER on 13^{th} March 2010.

2.2 Frequency and time characteristics

The DEMETER ICE experiment detected ~~terrestrial~~ kilometric wave emissions in the frequency range between few kilohertz and up to 800 kHz. ~~Fig.1 shows a dynamic spectrum recorded by ICE experiment on 10^{th} January 2010 between 13:58 UT and 14:06 UT. The satellite was on the late evening sector, around 22 LT, at a distance of 665 km. In this time interval the satellite geographical coordinate varied from -18°S to +04°N in latitude and 142° to 138° in longitude. We distinguish two varieties of kilometric emissions as indicated with arrows on Fig.1. The first radiation is called hereafter Type 1, and it appears as~~ Two examples recorded on the night-side are shown in Fig.1 and Fig.2. First panel of Fig.1 displays the dynamic spectrum recorded by ICE experiment on 21^{st} Feb. 2010 between 13:52 UT and 14:12 UT. The satellite was on the late evening sector, around 22 LT, at a distance of 665 km. In this time interval the satellite geographical coordinate varied from -18°S to +04°N in latitude and 142° to 138° in longitude. The second event shown in the first panel of Fig.2 was also recorded at about 22 LT

at similar distance from the Earth. Satellite geographical coordinate varied from -25°S to 40°N in latitude and 117° to 102° in longitude in the time interval between 14:10 UT and 14:26 UT. Second panel of Fig.1/Fig.2 displays a zoomed part of the dynamic spectrum shown in the first panel where the kilometric wave emission appears in the frequency range between few kHz and up to 800 kHz. One note on both second panels of Fig.1 and Fig.2, changes in the spectral kilometric wave emissions before and after 50 kHz. Hence the first radiation appears as a narrow continuum with an instantaneous bandwidth of about 2 kHz at frequencies less than 50 kHz. ~~Type 1~~ It displays negative and positive frequency drifts when the satellite is approaching or leaving the equatorial plane, respectively. Its frequency drift rate is weak and in the order of 0.2 kHz/s. The second emission is ~~called Type 2 and it~~ is composed of parallel narrow-bands, ~~as shown in Fig.1,~~ in a frequency above 50 kHz and up to 800 kHz. The band time duration is, on average, of about 1 minute and decreases to less than one minute when the emission frequency increases. The frequency bandwidth varies from few kHz and up to 20 kHz. Some narrow-bands showed a high power level (red color in Fig.1/Fig.2) when they are compared to other narrow bands. Those enhanced emission bands exhibit an extensive time duration of about 3 minutes.

2.3 Magnetic latitude and power level occurrence

The ~~terrestrial~~ kilometric wave radiation occurrences in magnetic latitude and power level are shown, respectively, in the top and the bottom panels of ~~Fig.2~~ Fig.3. The main kilometric emission were recorded when DEMETER was in the southern part of the magnetic equatorial plane. Hence the emissions are detected in the magnetic latitude range between -40° and 20°, as shown in the first panel of ~~Fig.2~~ Fig.3. We note a clear progressive increase of the kilometric emission occurrence which reaches a maximum at magnetic latitude of -10°. More than 90% of the kilometric radiation occurred in magnetic latitude range between -50° and 0°. Sudden decrease of the occurrence is recorded when the satellite crosses the magnetic equatorial plane. Emission is found to be more extended in the southern hemisphere with a clear di–symmetry occurrence before and after the equatorial magnetic plane.

The power level, as displayed in the second panel of ~~Fig.2~~ Fig.3, is covering a large interval between 10^{-3} ~~$\mu Vm^{-2}Hz^{-1}$~~ $\mu Vm^{-1}Hz^{-1/2}$ and 10^{+4} ~~$\mu Vm^{-2}Hz^{-1}$~~ $\mu Vm^{-1}Hz^{-1/2}$. More than 70% of the ~~terrestrial~~ $\mu Vm^{-1}Hz^{-1/2}$ emissions have a level less than 1 ~~$\mu Vm^{-2}Hz^{-1}$~~ and belong mainly to the southern hemisphere. Above this weak power level, the occurrence of ~~terrestrial~~ kilometric emission is associated to both hemispheres. The intense power level is associated to the kilometric emission occurring mainly at lower frequency, i.e. from few kilohertz and up to 100 kHz ~~(see sub-Section 2.4)~~. We distinguish three occurrence maxima at about 5x 10^{-3} ~~$\mu Vm^{-2}Hz^{-1}$~~ $\mu Vm^{-1}Hz^{-1/2}$, 1 ~~$\mu Vm^{-2}Hz^{-1}$~~ $\mu Vm^{-1}Hz^{-1/2}$ and 80 ~~$\mu Vm^{-2}Hz^{-1}$~~ $\mu Vm^{-1}Hz^{-1/2}$. We separate the power level by taking into consideration the interval associated to the previous maxima. Hereafter green, blue and red colors indicate, respectively, three power level intervals, i.e. 0.001 - 0.7 ~~$\mu Vm^{-2}Hz^{-1}$~~ $\mu Vm^{-1}Hz^{-1/2}$, 0.7 - 10 ~~$\mu Vm^{-2}Hz^{-1}$~~ $\mu Vm^{-1}Hz^{-1/2}$, and 10 - 10^4 ~~$\mu Vm^{-2}Hz^{-1}$~~ $\mu Vm^{-1}Hz^{-1/2}$.

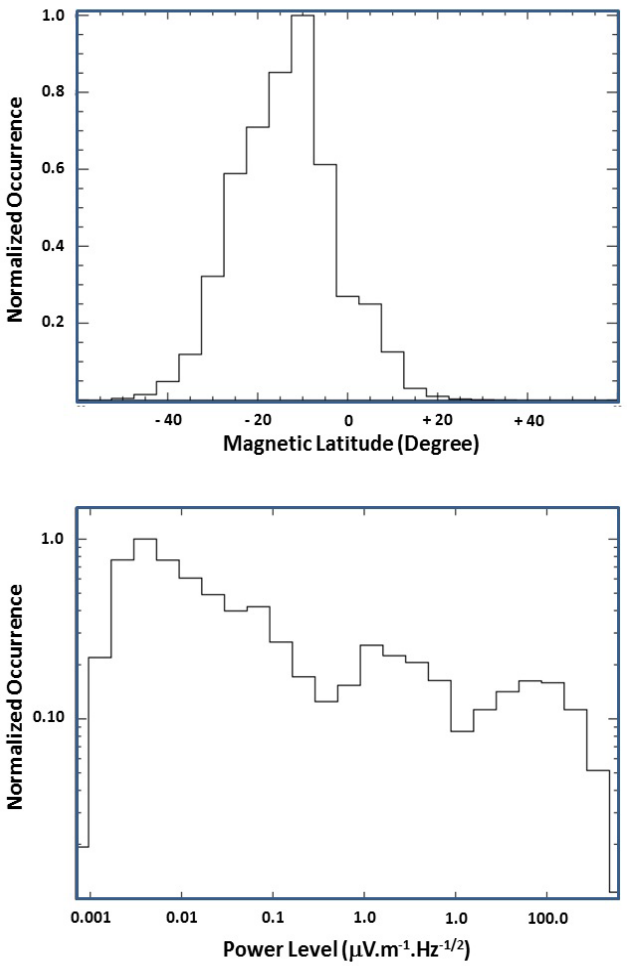

Figure 3. ~~Vertical lines indicate the occurrence of the kilometric emissions observed on 25th Feb. 2010. Those events were recorded on the night-side of the Earth with a time interval of about 01h35mnin. Green, blue and red colors specify, respectively, three power level intervals, i.e. 10^{-3} – 0.7 $\mu Vm^{-2}Hz^{-1}$~~, 0.7 - 10 ~~$\mu Vm^{-2}Hz^{-1}$~~, and 10 – 10^{+4} ~~$\mu Vm^{-2}Hz^{-1}$~~ Occurrence of kilometric wave emissions in magnetic latitude (Degree) and in power level ($\mu Vm^{-1}Hz^{-1/2}$).

Kilometric ~~radio~~ wave emissions are regularly observed on the nigh-side (22 LT) before and after the magnetic equatorial plane in the vicinity of the Earth at a distance less than 750 km. ~~Fig.3~~ Fig.4 displays the daily occurrence of kilometric radio emissions observed by ICE experiment on 25^{th}

Feb. 2010. We observe a periodic occurrence of the emission with a time interval of about 1h35 which corresponds to a DEMETER microsatellite full orbit. Each vertical line is considered as an 'event' and corresponds to the recorded emission for a given half-orbit. The occurrence per day is about 13 events in the optimal case. However from one event to another we ~~note~~ find a variation in the frequency bandwidth and also in the power level. ~~The lower part up to 50 kHz is mainly associated to the Type 1, and above this lower frequency limit we distinguish the Type 2 radiation which extended up to 500 kHz, and sometimes more.~~

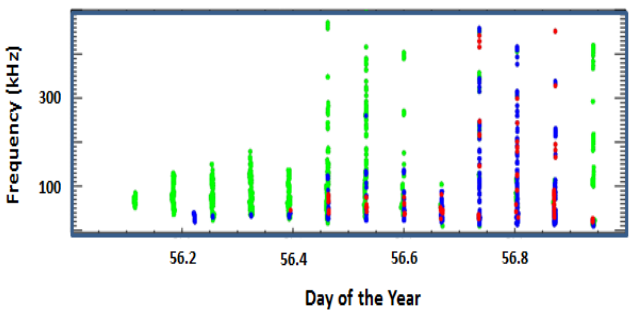

Figure 4. ~~Variation of the power levels versus the frequency (vertical axis) and the magnetic latitude (horizontal axis) for all events. Colors are similar to those used in Fig.3.~~ Vertical lines indicate the occurrence of the kilometric emissions observed on 25^{th} Feb. 2010. Those events were recorded on the night-side of the Earth with a time interval of about 01h35mnin. Green, blue and red colors specify, respectively, three power level intervals, i.e. $10^{-3} - 0.7\ \mu Vm^{-1}Hz^{-1/2}$, 0.7 - 10 $\mu Vm^{-1}Hz^{-1/2}$, and $10 - 10^{+4}\ \mu Vm^{-1}Hz^{-1/2}$.

2.4 Power level versus frequency and magnetic latitude

~~Fig.4~~ Fig.5 displays the power level variation versus the magnetic latitude where the colors indicate different power levels as defined in the previous sub-Section. The weakest intensities (less than 0.7 ~~$\mu Vm^{-2}Hz^{-1}$~~ $\mu Vm^{-1}Hz^{-1/2}$) are recorded at magnetic latitudes between -50° and +30° but much more in the southern hemisphere, as displayed in first panel of ~~Fig.4~~ Fig.5. Structured emissions appear when the magnetic latitude is positive principally after the crossing of the magnetic equatorial plane. One can distinguish five components appearing in four frequency ranges: few kHz - 50 kHz, 70 kHz - 130 kHz, 170 kHz - 250 kHz, 280 kHz -340 kHz and 380 kHz- 420 kHz. Those radiations are extended in magnetic latitudes in particular at low frequencies around 50 kHz, and decreases at higher frequencies, at about 400 kHz. ~~Terrestrial~~ Kilometric wave emission is quasi-absent between those four frequency bands.

Also structured emissions are observed in the southern part of the magnetic equatorial plane at frequencies above 200 kHz in magnetic latitude between -10° and 0° degrees, as shown in the first panel of ~~Fig.4~~ Fig.5. Those structures are mainly extended in frequency, contrary to those observed in northern hemisphere which extended in magnetic latitude. We distinguish four components occurring in the following frequency bands: 200 kHz - 320 kHz, 320 kHz - 450 kHz, 450 kHz - 570 kHz and 570 kHz - 670 kHz. At frequencies lower than 200 kHz, we note a quasi-absent of structured emission in the southern hemisphere. ~~Terrestrial~~ Kilometric ~~emissions~~ radiation continuously occur in magnetic latitude between -50° and 0°. In this interval, we find a positive/negative frequency drift rate of about +3.75 / -1. 25 kHz/degree when the frequency is higher/smaller than 50 kHz. The ~~terrestrial~~ kilometric emissions is mainly confined to frequencies lower than 150/100 kHz in the southern/northern part of the magnetic equatorial plane when the power level is between 0.7 and 10 ~~$\mu Vm^{-2}Hz^{-1}$~~ $\mu Vm^{-1}Hz^{-1/2}$, as displayed in the second panel of ~~Fig.4~~ Fig.5. Above 150 kHz, the radiations only occur in the frequency bandwidth 180 kHz to about 250 kHz. The power level in the range 10 - 10^4 ~~$\mu Vm^{-2}Hz^{-1}$~~ $\mu Vm^{-1}Hz^{-1/2}$ is shown in the third panel of ~~Fig.4~~ Fig.5. The main ~~terrestrial kilometric~~ emission is nearly symmetrical distributed around the magnetic equatorial plane, between -10° and +10°, predominantly above 100 kHz. Below this limit, the radiation covers larger magnitude latitude from -20° to about +20°.

The overlapping of the three power levels, as shown in ~~Fig.5~~ Fig.6, allow getting a global shape ~~of the so-called~~ similar to a 'Christmas-tree' pattern. We see globally that the kilometric emission is extensively occurring at frequency lower than 150 kHz, and starts to be less confined to the magnetic equatorial plane above this frequency limit. A cut-off appears around 50 kHz which decreases to about few kHz when approaching the magnetic equator plane. This cut-off is characterized by a small frequency drift rate in latitude and a power level in the interval 0.7 and 10 ~~$\mu Vm^{-2}Hz^{-1}$~~ $\mu Vm^{-1}Hz^{-1/2}$, i.e. blue color boundary in ~~Fig.5~~ Fig.6. A second cut-off can be seen when the DEMETER satellite was in the southern hemisphere and absent in northern hemisphere. It starts at latitudes of about -40° and disappears at -18° when the frequency decreases from 150 kHz to 50 kHz. We find that both cut-offs intersected at frequency of about 50 kHz when the magnitude latitude is about -18°.

3 Discussion

We discuss hereafter the kilometric ~~radiation~~ wave emission as detected by the DEMETER microsatellite. First we emphasis on the ~~spectral features where we show that similar emissions were recorded by previous satellite at close distance to the Earth but not regularly as allow the DEMETER orbits. Second we discuss the beaming of the kilometric emission taking into consideration its extension~~

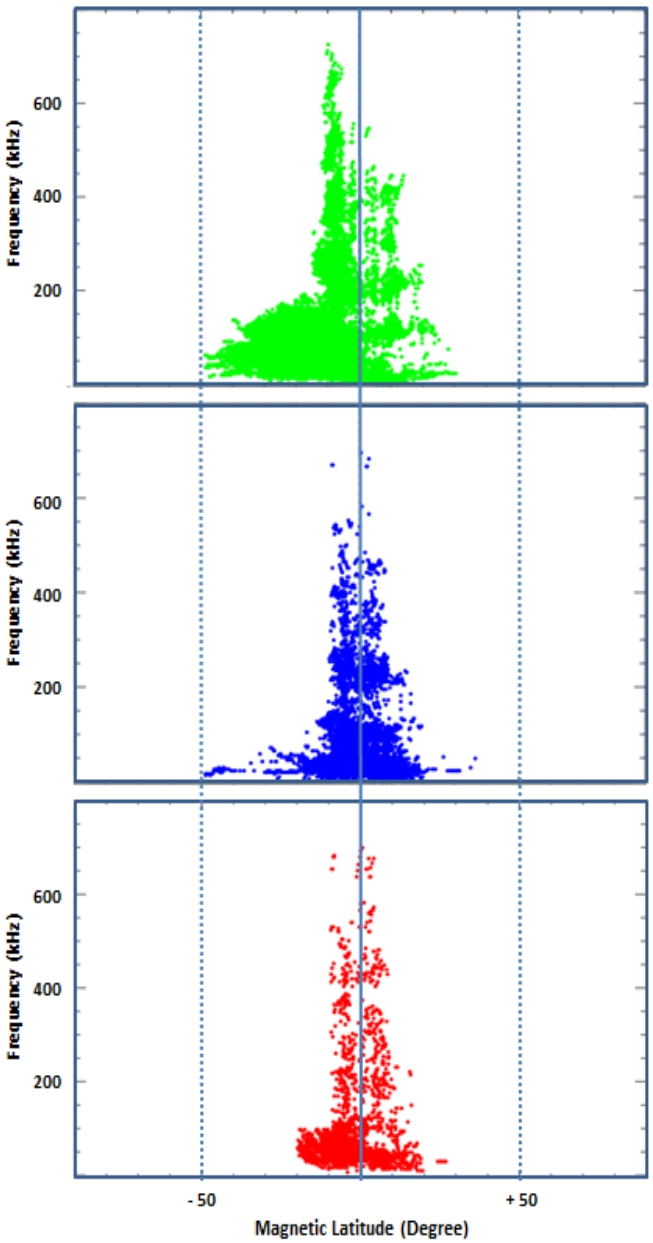

Figure 5. Overlapping of the three power levels displayed in Fig.4. The so-called 'Christmas tree' pattern appears around the magnetic equatorial plane Variation of the power levels versus the frequency (vertical axis) and the magnetic latitude (horizontal axis) for all events. Colors are similar to those used in Fig.4. Green, blue and red colors specify, respectively, three power level intervals, i.e. $10^{-3} - 0.7\ \mu V m^{-1} Hz^{-1/2}$, 0.7 - 10 $\mu V m^{-1} Hz^{-1/2}$, and $10 - 10^{+4}\ \mu V m^{-1} Hz^{-1/2}$.

in magnetic latitude and its dependence on frequency. Finally, we attempt to localize the source origins where the plasmasphere can be considered as the main location of such emission beaming of such emissions and how it extended and restrained around the magnetic equatorial plane. Then the similarity and the discrepancy between DEMETER kilometric emission and the terrestrial kilometric radiations are addressed. This is followed by a discussion on the generation mode and the source location.

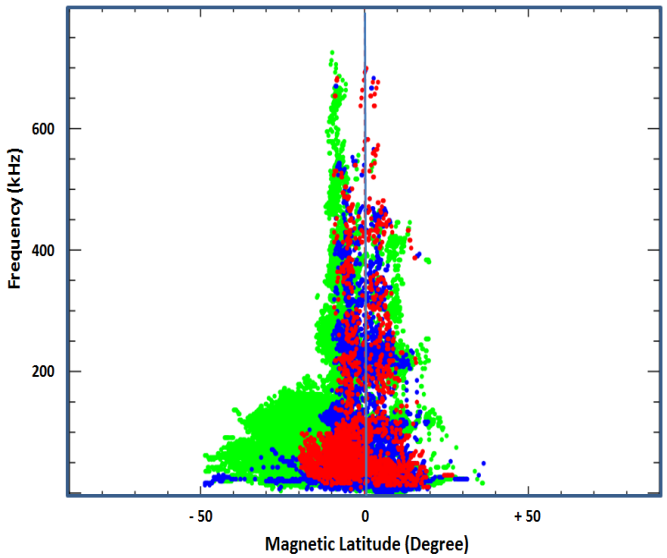

Figure 6. Variation of the terrestrial kilometric emissions versus the L-Shell and the magnetic latitude Overlapping of the three power levels displayed in Fig.5. The spectral pattern looks like a 'Christmas tree' with a 'trunk' along the magnetic equatorial plane.

3.1 Spectral features of kilometric emissionsBeaming of the kilometric wave emission

The passage of DEMETER satellite through the magnetic equator allowed re-discovering the terrestrial kilometric radiation. The recorded emissions are similar to those observed by other satellites, like Cluster, GEOTAIL and IMAGE. Hence the two types were also recorded and described in the literature. However the main advantage of DEMETER is its low altitude which was of about 700 km and regular observations of the kilometric emissions. Both components were reported and described as trapped and escaping emissions corresponding, respectively, to Type 1 and Type 2. Of course the spectral features are often comparable and the main alternations may be due to the instrumental time and frequency resolutions, and also the satellite orbits with regard to the source locations. DEMETER recorded emissions on both side of the magnetic equator, and they appear to be more structured in the northern hemisphere. Such frequency patterns may be related to the source regions which should be the plasmasphere. Those lasting bands indicate a 'stable' features in the late evening sector of the plasmasphere, i.e. at about 22 LT.

~~The parallel narrow bands are mainly associated to the escaping continuum. Green and Boardsen (2006) show a typical example of the kilometric continuum recorded by RPI/IMAGE experiment during a passage of the magnetic equator plane. AKR-X/INTERBALL-1 experiment provided similar emissions particularly in the southern hemisphere at low magnetic latitude and at L-Shell of about 1.2 (Kuril'chik et al., 2001). Observations at fixed frequencies (100 kHz, 252 kHz, 500 kHz and 749 kHz) allowed the analysis of the spectral character of such emissions. Authors showed that the terrestrial kilometric radiation occurrence is depending on the solar activity. Such radiation is regularly recorded during quiet solar activity. Our observations were registered in the begging of the year 2010, nearly eighteen months after the minimum of solar activity, i.e. Aug. 20008.~~

The passage of DEMETER satellite through the magnetic equator lead to characterize a kilometric radiation recorded in the vicinity of the magnetic equatorial plane. The capability of DEMETER satellite leads to regularly recorded such type of emission at low altitudes around 700 km. We have found that the kilometric radiations exhibit different spectral patterns when the frequency is smaller or bigger than 50 kHz. The satellite recorded emissions on both side of the magnetic equator, and they appear to be more structured bands in the northern hemisphere. Those lasting bands indicate a 'stable' features in the late evening sector at about 22 LT.

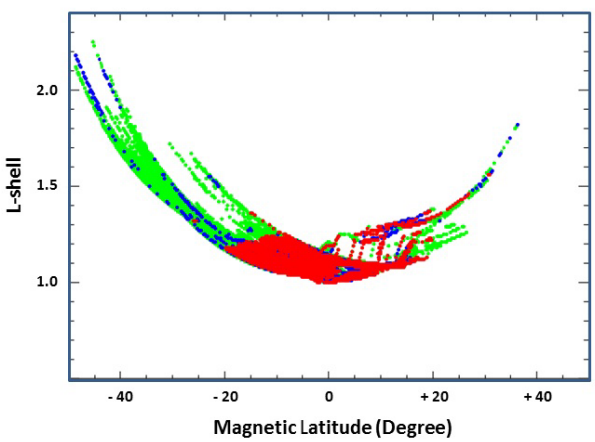

Figure 7. ~~Sketch of the beams observed in the southern (blue color) and the northern (red color) parts of the magnetic equator plane, as resulting from Fig4b. The strong power levels (green-dark color) are recorded at $\pm 10°$ magnetic latitude~~ Variation of the terrestrial kilometric emissions versus the L-Shell and the magnetic latitude.

The power level distribution of the kilometric emission shows restrained and extended deployment around the equatorial magnetic plane. Hence the latitudinal beam is found to be of about 40° when the frequency is, on average, less than 100 kHz. Above this limit and up to about 800 kHz, the latitudinal beam is decreasing and found of about 20°. This general picture is easily seen in the third panel of Fig.5. However we note a clear difference in the beam when the level is less than 1 $\mu V m^{-1} Hz^{-1/2}$, as showed in the first panel of Fig.5. Hence the kilometric wave radiation beam is different when combing the emission recorded in the southern and northern parts of the magnetic equatorial plane. In the southern one, half of the spectral pattern is observed, i.e. beams of 25° and 10°, on average, in the frequency bandwidths 30 kHz-100 kHz and 100 kHz-800 kHz, respectively. On the other side of the equatorial magnetic plane only branches, or limbs, are detected as shown in the first panel of Fig.5. It is evident that emission diagrams are unlike which may be due to combine effects of multi-sources locations and ray path propagations.

The beams of the kilometric events are found to depend on the satellite orbits with regard to the magnetic equatorial plane. The two beams associated to the southern hemisphere events are observed in different frequency bandwidth. We may be deal with two source regions localized in the southern part of the magnetic equator but confined to two unlike regions with high and low plasma densities. Fig.7 displays the variation of the L-shell associated to the kilometric events versus magnetic latitude of the satellite. The power level is principally found to increase between 1 and 1.4 L-shell when the magnetic latitude of DEMETER is in between -20° and +20°. The source locations of kilometric wave radiation seem to be confined to a narrow L-shell region.

Fig.8 provides a sketch of the emission diagrams of the kilometric wave emissions. Those diagrams are different before and after the magnetic equatorial plane. Hollow cones may be considered in the 'southern' source emission with opening angle which is small at frequency of about 700 kHz and increase to 40° around 100 kHz. Multi-beams can be related to the 'northern' sources which looks like a succession of 'laser-beams' emitting at specific frequencies.

3.2 ~~Beaming and source locations of kilometric emissions~~Similarity and discrepancy with the terrestrial kilometric emission

~~The power level distribution of the kilometric emission shows restrained and extended deployment around the equatorial magnetic plane. Hence the latitudinal beam is found to be of about 40° when the frequency is, on average, less than 100 kHz. Above this limit and up to about 800 kHz, the latitudinal beam is decreasing and found of about 20°. This general picture is easily seen in the third panel of Fig.4. However we note a clear difference in the beam when the level is less than 1 $\mu V m^{-2} Hz^{-1}$, as one can see in the first panel of Fig.4. Hence the terrestrial kilometric beam is different when combing the emission recorded in the southern and northern parts of the magnetic equatorial plane. In the southern one, half of the Christmas-tree pattern is observed, i.e. beams of 25° and 10°, on average, in the frequency bandwidths 30 kHz-100 kHz and 100 kHz-800 kHz, respectively. On the other side of the equatorial~~

magnetic plane only branches, or limbs, are detected as shown in the first panel of Fig.4. It is evident that emission diagrams are unlike which may be due to combine effects of multi-sources locations and ray path propagations.

The beams of the terrestrial kilometric events are found to depend on the satellite orbits with regard to the magnetic equatorial plane. The two beams associated to the southern hemisphere events are observed in different frequency bandwidth. We may be deal with two source regions localized in the southern part of the magnetic equator but confined to two unlike regions with high and low plasma densities. Fig.6 displays the variation of the L-shell associated to the terrestrial kilometric events versus magnetic latitude of the satellite. The power level is principally found to increase between 1 and 1.4 L-shell when the magnetic latitude of DEMETER is in between -20° and +20°. The source locations of terrestrial kilometric radiation seem to be confined to a narrow L-shell region.

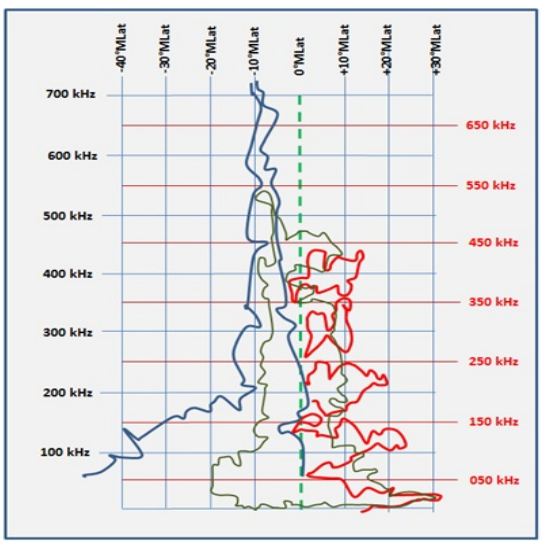

Figure 8. EUV IMAGE observations of the Earth's plasmasphere as reported by Sandel et al (2003). The time evolution of the plume structure is shown with the yellow color Sketch of the beams observed in the southern (blue color) and the northern (red color) parts of the magnetic equator plane, as resulting from Fig.6. The strong power levels (green-dark color) are recorded at $\pm 10^{\circ}$ magnetic latitude.

Fig.7 provides a sketch of the emission diagrams of the terrestrial kilometric emissions. Those diagrams are different before and after the magnetic equatorial plane. Hollow cones may be considered in the 'southern' source emission with opening angle which is small at frequency of about 700 kHz and increase to 40° around 100 kHz. Multi-beams can be related to the 'northern' sources which looks like a succession of 'laser-beams' emitting at specific frequencies. Southern and northern sources are probably localized in the plasmasphere, as suggested by previous studies (see review of Green et al., 2004). The physical process is depending on the source plasma conditions and the strength of the Earth's magnetic field. Kuril'chik al. (2001) addressed this physical process by considering the presence of Z and LO escaping modes.

Kilometric wave emission features, as investigated in this paper, allow us to address questions concerning its origin. We have found some spectral patterns which are similar to those reported in the literature in the case of the terrestrial kilometric emissions.

First, we have described changes of the spectral kilometric emissions at frequencies of about 50 kHz. Such frequencies boundaries are similar to those observed by other satellite observations, like Cluster, GEOTAIL and IMAGE. Hence the terrestrial kilometric radiation is trapped and escaping when the frequency is, respectively, smaller and bigger than 50 kHz. The spectral features are often comparable and the main alternations may be due to the instrumental time and frequency resolutions, and also the satellite orbits with regard to the source locations. For example, the parallel narrow bands as displayed in Fig.5 are mainly associated to the escaping continuum in the case of the terrestrial kilometric emission. Hence Green and Boardsen (2006) show a typical sample of the kilometric continuum recorded by RPI/IMAGE experiment during a passage of the magnetic equator plane. AKR-X/INTERBALL-1 experiment provided similar emissions particularly in the southern hemisphere at low magnetic latitude and at L-Shell of about 1.2 (Kuril'chik et al., 2001). Observations at fixed frequencies (100 kHz, 252 kHz, 500 kHz and 749 kHz) allowed the analysis of the spectral character of such emissions. Authors showed that the terrestrial kilometric radiation occurrence is depending on the solar activity. Such radiation is regularly recorded during quiet solar activity. Our observations were registered in the begging of the year 2010, nearly eighteen months after the minimum of solar activity, i.e. Aug. 2008. Also the spectral pattern looks like a 'Christmas-tree' as also reported by Green and Boardsen (2006) in their review about the kilometric continuum radiation and it is confined to the magnetic equatorial plane.

Despite those common spectral features, several other observational aspects are different when combining the terrestrial kilometric radiation and the kilometric wave emission. The investigated DEMETER emission is detected at distance of about $1.1R_E$ which is generally not the case of the terrestrial kilometric emission. For instance GEOTAIL and CLUSTER observations recorded radiation at more than $15R_E$ as reported by Hashimoto et al. (1999) and (Décréau et al., 2004), respectively. Also, the trapped or the escaping component is linked to terrestrial kilometric radiation recorded,respectively, between the plasmasphere and the magnetosphere, or outside of the magnetosphere. This radiation propagate largely in the free space in the L-O mode above the local plasma frequency linked to sources at or

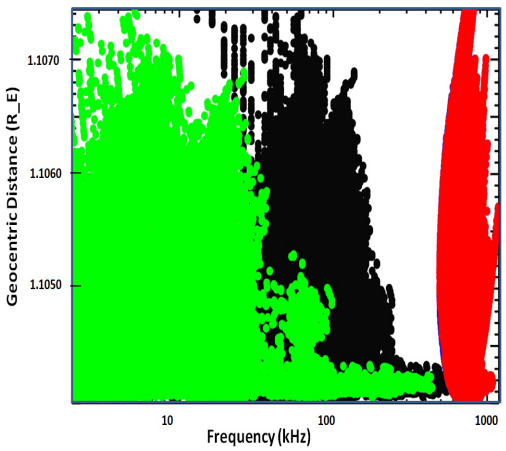

Figure 9. Variations of the kilometric wave emission versus the geocentric distance expressed in R_E. The green, black and red colors are associated, respectively, to f_z, f_p and f_g frequencies.

very near the plasmapause (Hashimoto et al., 2006). Also the gyro-frequency is found to be smaller than the trapped and the escaping frequencies as recorded by RPI/IMAGE experiment (see Fig.2 of Green and Boardsen (2006)). All those observational parameters are not similar to those reported in the case of the kilometric wave emission recorded by DEMETER satellite.

3.3 ~~Morphological aspects of the plasmasphere~~ Micro-scale features of the inner part of the plasmasphere

~~IMAGE scientists reported about density structures recorded by EUV experiment (Burch et al., 2000). Such structures have been discovered by combing IMAGE and Clusters observations. New terms have been defined like channels, crenulations, fingers and shoulders as reviewed in Darrouzet et al.(2009). We consider hereafter the work of Sandel et al. (2003) who investigated a plasmaspheric event observed on 10^{th} June 2001 using EUV IMAGE observations. The so-called 'Christmas-tree' pattern with different emission diagrams, before and after magnetic equatorial plane, may be compared to the mechanism that can create channel. Fig.8 shows a time evolution of the pre-midnight sector when a drainage plume wrapped around the plasmasphere for the event of 10^{th} June 2001. In the left panel of Fig.8 Sandel et al (2003) found that the inner part of the plume corotates when the outer parts remain fixed in local time. Four hours later, as seen in the middle panel, the plume starts to wrap around the plasmasphere. After nine hours, the base of the plume has drifted westward in longitude and channel appears between the plume and the main body of the plasmasphere, as displays in the right panel of Fig.8. The DEMETER observations of the terrestrial kilometric emissions provided similar outcomes in particular in the final phase where the channel is generated. We can consider that the plume and the channel are comparable to the kilometric radiation beaming observed before and after the magnetic equatorial plane, respectively. The plume development in the azimuthal plane, as described by EUV IMAGE, has a complement part in the latitudinal plane. In the pre-midnight part of the plasmasphere, the generations of channels, and fingers, may be associated to the 'laser-beams' recorded by DEMETER~~.

It is clear that both radiations have common spectral features but several discrepancy observational aspects linked to the generation mechanism. However the source locations should be the plasmasphere. Hence the terrestrial kilometric radiation is linked to plasmaspheric sources with emission beams oriented towards the magnetosphere. However the beaming of the DEMETER kilometric wave emissions is towards the Earth's ionosphere with sources localized in the plasmasphere. It is important to note that the DEMETER kilometric events belongs to a very limited regions in range 1-2 L-Shell (as shown in Fig.7) with distances between $1.1040R_E$ and $1.1070R_E$. This means that the DEMETER orbits is crossing the plasmaspheric hollow cones on few dozen of kilometer. Probably such restricted regions may be associated to the Z-mode waves which are linked to the free escaping L-O mode as suggested by Jones (1976) in his model. In such region the Z-mode waves are considered to be trapped and later converted into L-O mode associated to the terrestrial kilometric radiation. Green and Boardsen (2006) investigated and reported about the linear mode conversion theory based on Jones model. Authors showed profiles of plasmaspheric plasma frequency taking into consideration the Z-mode and the equatorial gyro-frequency. Regions of sharp plasma gradient are found and shown in Fig.5 of their paper. Carpenter et al. (2003) found similar region where ray paths of Z-mode echoes from radio sounding were recorded by IMAGE satellite in the polar regions.

We estimate the relationship between the Z-mode frequency (f_z), the plasma frequency (f_p) and the gyro-frequency (f_g) using the following formulae: $f_z = (f_g/2)[-1 + (1 + 4(f_p/f_g)^2)^{1/2}]$ (Carpenter et al., 2003). Fig.9 displays the variation of the three frequencies (i.e. f_z, f_p and f_g) versus the geocentric distance. The trapping region is localized between the lower and the higher f_z (green color in Fig.9) mainly between 1 kHz and 100 kHz, and extended up to 700 kHz. The plasma frequency is following the trapping region and starting at about 10 kHz and up to 800 kHz. The gyro-frequency appears at higher frequencies, i.e. above 800 kHz. Those features are comparable to previous investigations, e.g. Gurnett and Shaw (1983) and Carpenter et al. (2003) but in other regions.

4 Conclusion

We have investigated the ~~terrestrial~~ kilometric wave radiation recorded by ~~ICE experiment onboard DEMETER satellite. We have distinguished two spectral types which are found to be linked to the 'trapped' and 'escaping' kilometric emission, as previously observed by several satellites~~ICE/DEMETER experiment. DEMETER orbits allow us to regularly record the ~~terrestrial emission. The occurrence per day is about 13 events in the optimal case~~kilometric radiation where, in the optimal case, about 13 events are daily registered. The power level is found in the interval between 10^{-3} $\mu Vm^{-2}Hz^{-1}\mu Vm^{-1}Hz^{-1/2}$ and 10^{+4} $\mu Vm^{-2}Hz^{-1}\mu Vm^{-1}Hz^{-1/2}$. The spectral analysis leads to ~~re-construct the so-called~~find a 'Christmas-tree' which is the traces of the beaming of the ~~terrestrial~~ kilometric wave radiation. We have shown that those beams are not similar and depend on the emission frequency and the magnetic latitude. ~~The emission sources are found to be mainly localized in the southern and also in the northern part of the magnetic equator plane. Further analysis allows finding that 'Christmas-tree' pattern may be considered to be related to the EUV temporal evolution of the pre-midnight sector of the plasmasphere where the plume structure ended with the generation of the so-called channel~~DEMETER kilometric emission can be comparable to the well-know terrestrial kilometric radiation. However several other observational aspects are different when combining both emissions in particular the generation modes. We suggest that the DEMETER kilometric emissions are linked to a Z-mode micro-scale region. This trapping Z-mode region can only be detected between the Earth's ionosphere and the plasmasphere. The hollow cones of this kilometric wave emissions are crossed by the DEMETER orbits at altitudes lower than 700 km. Probably the source regions of the DEMETER kilometric emission should be the plasmasphere, like the terrestrial kilometric radiation. IMAGE investigations reported about density structures recorded by EUV experiment (Burch et al., 2000) where new terms have been defined like channels and crenulations (Darrouzet et al., 2009), and also a time evolution of the plasmasphere in particular on the pre-midnight sector (Sandel et al., 2003). We may consider that DEMETER orbits allow to investigate the inner part of the plasmasphere when other missions (i.e. GEOTAIL, IMAGE, INTERBALL) lead to study the outer part of the plasmasphere.

Acknowledgements. Acknowledgements. We acknowledge C. N. E. S. for the use of the DEMETER data, and thankful to Jean-Jacques Berthelier who provided us with data from the electric field experiment (Instrument Champ Électrique – ICE).

References

Berthelier, J.J., Godefroy, M., Leblanc, F., Malingre, M., Menvielle, M., Lagoutte, D., Brochot, J.Y., Colin, F., Elie, F., Legendre, C., Zamora, P., Benoist, D., Chapuis, Y., Artru, J., and Pfaff, R.: ICE, the electric field experiment on DEMETER, Planet. Space Sci., 54, 456–471, 2006.

Boudjada, M.Y., Biagi, P.F., Al-Haddad, E., Galopeau, P.H.M., Besser, B., Wolbang, D., Prattes, G., Eichelberger, H., Stangl, G., Parrot, M., and Schwingenschuh, K.: Reception conditions of low frequency (LF) transmitter signals onboard DEMETER micro-satellite, Physics and Chemistry of the Earth, 102, 70–79, 2017.

~~Boudjada, M.Y., Sawas, S., Galopeau, P.H.M., Berthelier, J.J., and Schwingenschuh, K.; Study of AKR hollow pattern characteristics at sub-auroral regions, European Geosciences General Assembly, Vienna, 2014.~~

~~Boudjada, M.Y., Galopeau, P.H.M., Berthelier, J.J., Rucker, H.O., Kuril'chik, V.N., and Schwingenschuh, K.: Case studies of terrestrial kilometric and hectometric emissions observed by Demeter/ICE experiment, European Geosciences General Assembly, Vienna, 2009.~~

Brown, L.W.: The galactic radio spectrum between 130 kHz and 2600 kHz, Astrophys. J., 359–370, 1973.

Burch, J.L.: IMAGE mission overview, Space Sci. Rev., 91, 1–14, 2000.

Carpenter, D.L., Bell, T.F., Inan, U.S., Benson, R.F., Sonwalkar, V.S., Reinisch, B.W., and D. L. Gallagher, Z-mode sounding within propagation "cavities" and other inner magnetospheric regions by the RPI instrument on the IMAGE satellite, J. Geophys. Res., 108, A12, 2003.

Darrouzet, F., Gallagher, D. L., André, N., Carpenter, D. L., Dandouras, I., Décréau, P. M. E., De Keyser, J., Denton, R. E., Foster, J. C., Goldstein, J., Moldwin, M. B., Reinisch, B. W., Sandel, B. R., and Tu, J.: Plasmaspheric Density Structures and Dynamics: Properties Observed by the CLUSTER and IMAGE Missions, Space Sci. Rev., 145, 55–106, 2009.

Décréau, P. M. E., Ducoin, C., Le Rouzic, G., Randriamboarison, O., Rauch, J.-L., Trotignon, J.-G., Vallières, X., Canu, P., Darrouzet, F., Gough, M. P., Buckley, A. M., and Carozzi, T.D.: Observation of continuum radiations from the Cluster fleet: first results from direction finding, Ann. Geophys., 22, 2607-2624, 2004.

Décréau, P.M.E., Fergeau, P., Krasnoselskikh, V., Le Guirriec, E., Lévêque, M., Martin, Ph., Randriamboarison, O., Rauch, J.L., Senée, F. X., Séran, H.C., Trotignon, J.G., Canu, P., Cornilleau, N., de Féraudy, H., Alleyne, H., Yearby, K., Mögensen, P.B., Gustafsson, G., André, M., Gurnett, D.C., Darrouzet, F., Lemaire, J., Harvey, C.C., Travnicek, P., and Whisper experimenters: Early results from the Whisper instrument on Cluster: an overview, Ann. Geophys., 19, 1241-1258, 2001.

El–Lemdani Mazouz, F., Rauch, J.L., Décréau, P.M.E., Trotignon, J.G., Vallières, X., Darrouzet, F., Canu, P., and Suraud, X., Wave emissions at half electron gyroharmonics in the equatorial plasmasphere region: CLUSTER observations and statistics, Adv. Space Res., 43, 253-264, 2009.

Frankel, M.S.: LF radio noise from the earth's magnetosphere, Radio Sci., 8, 991-1005, 1973.

Green, J.L., and Boardsen, S.A.: Kilometric continuum radiation, Radio Sci. Bull., 318, 34- 41, 2006.

Green, J.L., Boardsen, S., Fung, S.F., Matsumoto, H., Hashimoto, K., Anderson, R.R., Sandel, B.R., and Reinisch, B.W.: Association of kilometric continuum radiation with plasmaspheric structures, J. Geophys. Res., 109, A03203, 2004.

Grimald, S., El-Lemdani Mazouz, F., Foullon, C., Décréau, P.M.E., Boardsen, S.A., and Vallières, X.: Study of non-thermal continuum patches: wave propagation and plasmapause study, J. Geophys. Res., 116, A07219, 2011.

Grimald, S., Décréau, P.M.E., Canu, P., Rochel, A., and Vallières, X.: Medium latitude sources of plasmaspheric non thermal continuum radiations observed close to harmonics of the electron gyrofrequency, J. Geophys. Res., 113, A11217, 2008.

Gurnett, D.A.: The Earth as a radio source: The nonthermal continuum, J. Geophys. Res., 80, 2751–2763, 1975.

Gurnett, D. A., and Frank, L.A.: Continuum radiation associated with low-energy electrons in the outer radiation zone, J. Geophys. Res., 81, 3875–3885, 1976.

Gurnett, D. A., and Shaw, R.A.: Electromagnetic radiation trapped in the magnetosphere above the plasma frequency, J. Geophys. Res., 78, 8136- 8148, 1973.

Gurnett, D. A., Shawhan, S.D., and R. R. Shaw, Auroral hiss, Z-mode radiation, and auroral kilometric radiation in the polar magnetosphere: DE 1 observations, J. Geophys. Res., 88, 329, 1983.

Gurnett, D.A., Calvert, W., Huff, R.L., Jones, D., and Siguira, M.: The polarization of escaping terrestrial continuum radiation, J. Geophys. Res., 93, 12817–12825, 1988.

Hashimoto, K., Green, J.L., Anderson, R.R., and Matsumoto, H.: Review of kilometric continuum, in Geospace Electromagnetic Waves and Radiation, Lect. Not. in Phys., Eds. J. W. LaBelle and R. A. Treumann, Springer, New York, 687, 37–54, 2006.

Hashimoto, K., Calvert, W., and Matsumoto, H.: Kilometric continuum detected by GEOTAIL, J. Geophys. Res., 104, 28,645-28,656, 1999.

Jones, D.: Source of terrestrial nonthermal radiation, Nature, 260, 686-689, 1976.

Jones, D., Mode-coupling of Z mode waves as a source of terrestrial kilometric and Jovian decametric radiations, Astron. & Astrophys., 55, 245–252, 1977.

Jones, D.: Beaming of terrestrial myriametric radiation, Adv. Space Res., 1,373, 1981.

Jones, D., Calvert, W., Gurnett, D.A., and Huff, R.L.: Observed beaming of terrestrial myriametric radiation, Nature, 328, 391, 1987.

Kuril'chik, V.N., Boudjada, M.Y., Rucker, H.O., and Kopaeva, I.F.: Observations of Electromagnetic Emissions inside the Earth's Plasmasphere from the INTERBALL-1 Satellite, Cosmic Res., 45, 455–460, 2007.

Kuril'chik, V.N, Boudjada, M.Y, and Rucker, H.O.: The Observations of the Subauroral Nonthermal Radio Emission by AKR-X Receiver onboard of the INTERBALL Satellite, in Planetary Radio Emissions V, edited by: Rucker, H.O., Kaiser, M.L., and Leblanc, Y., Austrian Academy of Sciences Press, Vienna, Austria, 202–212, 2001.

Kurth, W.S., Gurnett, D.A., and Anderson, R.R.: Escaping nonthermal continuum radiation, J. Geophys. Res., 86, 5519–5531, 1981.

Parrot, M., and Berthelier, J.J.: AKR-like emissions observed at low altitude by the DEMETER satellite, J. Geophys. Res., 117, A10314, 2012.

Parrot, M., Inan, U.S., Lehtinen, N.G., and Pincon, J.L.: Penetration of lightning MF signals to the upper ionosphere over VLF ground-based transmitters, J. Geophys. Res., 114, A12318, 2009.

Sandel, B.R., Goldstein, J., Gallagher, D.L., and Spasojevic, M.: Extreme ultraviolet imager observations of the structure and dynamics of the plasmasphere. Space Sci. Rev., 109, 25-46 2003.